Effect of Ion-Wave Damping on Stimulated Raman Scattering in High-Z Laser-Produced Plasmas

R. K. Kirkwood,[1] B. J. MacGowan,[1] D. S. Montgomery,[1] B. B. Afeyan,[1] W. L. Kruer,[1] J. D. Moody,[1] K. G. Estabrook,[1] C. A. Back,[1] S. H. Glenzer,[1] M. A. Blain,[2] E. A. Williams,[1] R. L. Berger,[1] and B. F. Lasinski[1]

[1]*Lawrence Livermore National Laboratory, University of California, L-473 P.O. Box 808, Livermore, California 94550*

[2]*Centre D'Etudes de Limeil-Valkenton, France*

(Received 25 April 1996; revised manuscript received 1 August 1996)

The dependence of the magnitude of stimulated Raman scattering (SRS) on ion-wave damping has been demonstrated in a high-Z plasma. The ion-wave damping is varied in a well characterized Xe plasma by varying the concentration of a C_5H_{12} impurity. The reflectivity of SRS is observed to increase with the concentration of the dopant, demonstrating the effect of ion-wave damping on SRS. The measurements are consistent with models in which the amplitude of the SRS-driven Langmuir waves are limited by a secondary decay into ion-acoustic waves. [S0031-9007(96)01178-7]

PACS numbers: 52.40.Nk, 52.35.Mw

The transport of intense laser beams through large regions of under dense plasmas is important to the achievement of indirect drive inertial confinement fusion (ICF) [1]. The energy deposition profile of the laser beam in the target is strongly affected by stimulated scattering from ion acoustic and Langmuir waves in the plasma created when the target material ionizes. These interactions are most simply modeled by the three wave decay processes of stimulated Brillouin scattering (SBS) and stimulated Raman scattering (SRS), respectively [2]. However, previous experimental observations [3,4] and theoretical studies [5–13] provide evidence that the Langmuir waves and the ion acoustic waves are not independent. In fact, in the high-temperature, high-Z plasmas present in indirect drive targets [1] secondary decay instabilities can limit the SRS [9–13]. The SRS-driven Langmuir wave can decay into an ion acoustic wave and either a secondary Langmuir wave (LDI) or a secondary electromagnetic wave (EDI), thus coupling the properties of the Langmuir wave to the properties of the ion-acoustic wave directly. The mechanism for limiting SRS reflectivities by LDI was first described by Karttunen [9] and Heikkinen and Karttunen [10], and was later invoked to explain the SRS spectrum from Au foil plasmas [11]. These processes were subsequently shown to occur in numerical simulations [7,8,12]. Recently Baker [13] suggested that the EDI may also result in a limit to the reflectivity.

In this Letter we present the first demonstration that the SRS reflectivity in a plasma can depend directly on ion-wave damping, and find that the SRS reflectivity in our case is consistent with Langmuir wave amplitudes that are limited by a secondary decay. The experiments are done in a low density Xe gas target plasma, in which C_5H_{12} is added as a low-Z impurity. Measurements of x-ray spectra and transmitted light, and calculations all show that variation of the concentration of impurities below 10% has very little effect on the electron density, temperature, or collisional absorption rate, while calculations indicate the impurities have a large affect on the ion wave damping. The SRS reflectivity, or equivalently the Langmuir wave amplitude, is found to depend on the impurity concentration and thus on ion wave damping, and to track the threshold for decay of the Langmuir wave. The plasmas produced in these experiments mimic the properties of the plasma that forms near the wall in an Au *Hohlraum* filled with a low-Z gas such as will be used in ignition experiments (at lower laser intensity) [1], while providing a uniform and well characterized plasma. Other experiments in gas filled *Hohlraums* have also shown a dependence of SRS on ion wave damping both when the wall is doped with a Be impurity to mimic the gradients and time dependence of the wall plasma [14], and when the gas has large fractions of both low- and high-Z material [15]. However, plasma properties vary along the ray path in those experiments making identification of the physical mechanism difficult.

The experiments were carried out on the Nova laser facility in an approximately spherical plasma produced by nine $f/4.3$, $\lambda = 351$ nm beams. These heater beams each produce 2.5 TW of power continuously for 1 ns, with a total power of 22.5 TW. The beams pass through a gas mixture at 1 atm of pressure contained inside a 260 nm thick spherical polyimide shell with radius $r_0 = 1.3$ mm [16]. The heater beams are aligned to cross at the center of the target. The heaters are defocused such that they are converging with a beam radius that is approximately equal to the target radius, providing spatially uniform heating. The electrons are heated to a temperature of $T_e = 3.6$ keV during the $t = 0.5$ to 1.0 ns period when the plasma parameters are most constant in space and time [16]. The electron density is determined by the initial gas density and the average charge state. At this temperature Xe has a charge state of about 40 [17], leading to a density of $n = 8.5 \times 10^{20}$ cm^{-3}. Since the C_5H_{12} impurity is fully ionized and carries 42 electrons per molecule, the electron density is independent of its concentration to within $\leq 5\%$. The temperature is determined from measurements of x-ray line ratios and x-ray transport modeling as described in Ref. [17] and is in agreement with LASNEX

 0031-9007/96/77(13)/2706(4)$10.00

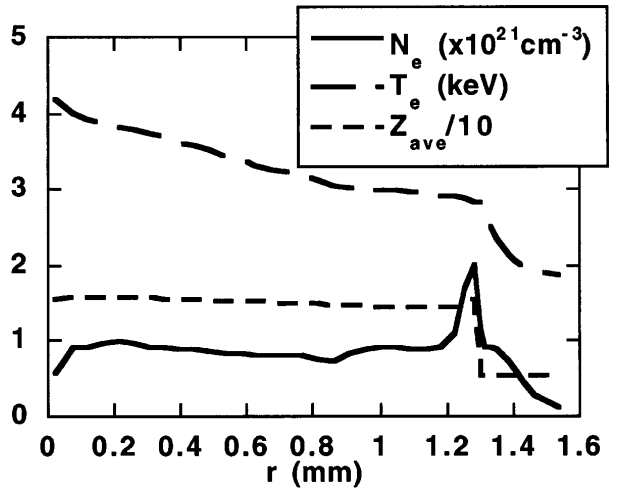

FIG. 1. Calculated electron density, temperature, and averaged ionization state at $t = 0.7$ ns indicate density and temperature scale lengths are long.

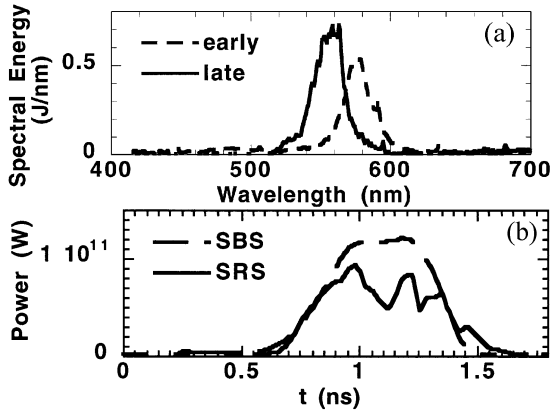

FIG. 2. (a) Time integrated reflectivity from a target with 5.5% impurity concentration shows a narrow peak at 575 nm in the 0.5 to 1.0 ns early period. (b) Spectrally integrated power collected by the SRS and SBS detectors is shown for the case in (a).

[18] simulations. Measurements of radiated power and beam attenuation by collisional absorption indicate that the temperature is insensitive to impurity concentration. The measured transmission of a beam through the plasma [19] varies only from 1% to 2% when the impurity concentration is varied from 0% to 30% and is in agreement with the simulations, similarly indicating that the electron temperature variations are small ($\leq \pm 6\%$). Measurements of the radiated x-ray power in the photon energy range of 0.2 to 2 keV [20] indicate that the radiated power is constant within $\pm 15\%$ over the same range of impurity concentration. The lack of dependence of the electron density and temperature on impurity concentration indicates that the frequency and damping rate of the Langmuir wave are constant.

An interaction beam produces 1.5 TW continuously for 1.0 ns with $\lambda = 351$ nm. This beam is delayed 0.5 ns with respect to the heaters and focused at the plasma center. Reflectivity measurements are made during the 0.5 to 1.0 ns (early) period when the heaters are on, as well as during the 1.0 to 1.5 ns (late) period when the plasma is cooling and less homogeneous. The interaction beam is smoothed by a random phase plate (RPP) and 0.7 Å FM bandwidth dispersed across the beam in the near field (SSD), so that its peak intensity and spot size in vacuum are 7.0×10^{15} W/cm^2 and 177 μm FWHM (345 μm between first Airy minima). The plasma properties encountered by the interaction beam during the early period are calculated by LASNEX [18] for a 90% Xe, 10% C_5H_{12} gas mix, indicating a temperature and density plateau near the plasma edge as shown in Fig. 1. The classical collisional absorption length for 351 nm light in Xe with a 3.6 keV electron temperature and 8.5×10^{20} cm^{-3} electron density is 800 μm. Therefore, the majority of the backscattering occurs outside $r = 0.5$ mm. The downshifted light scattered within 20° of direct backscatter [21] is measured with a streaked optical spectrometer in the visible, with a spectral range of 400 to 700 nm, and a second spectrometer in the UV, with a spectral range of 346 to 361 nm. The SRS light detected by the long wavelength spectrometer from an experiment with 5.5% C_5H_{12} impurity is shown in Fig. 2. During the early period the peak of the spectrum is at 575 nm consistent with scattering from a Langmuir wave propagating in a plasma with a density equal to 10% of the critical density and a 3.0 keV electron temperature comparable to the simulated plasma parameters near $r = 1.2$ mm. After the heaters turn off at 1.0 ns the peak shifts to the blue indicating cooling and expansion of the plasma.

Experiments were performed with six different impurity concentrations between 0% and 30% C_5H_{12} and exhibit a strong dependence of the SRS reflectivity on the

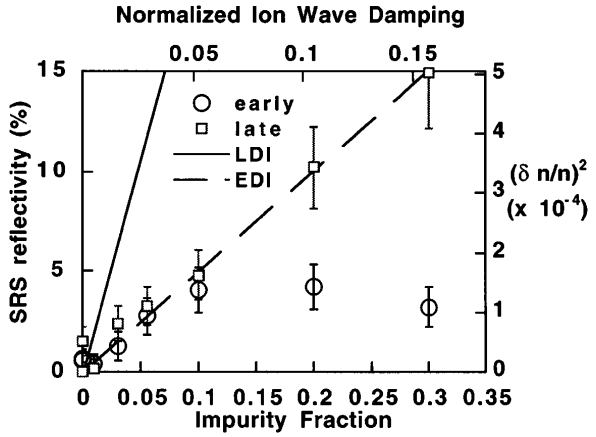

FIG. 3. SRS reflectivities averaged over the 0.5 to 1.0 ns early period and the 1.0 to 1.5 ns late period are shown vs. impurity concentration. The impurity concentration is interpreted as the ion-wave damping rate and the reflectivity is interpreted as the square of the fluctuation amplitude. Solid and dashed lines represent the EDI and LDI threshold amplitudes for a uniform beam and parameters relevant to early time data. The LDI limited reflectivity of a nonuniform beam can be much lower than what is shown as discussed in the text.

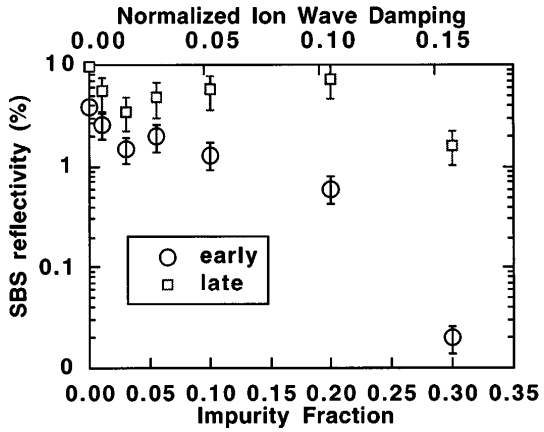

FIG. 4. SBS reflectivities for the same case as in Fig. 3. In the region of 3% to 10% impurity the SBS reflectivity does not decrease significantly, while the SRS reflectivity increases significantly.

concentration of C_5H_{12} which is interpreted as a dependence of Langmuir wave amplitude on the damping rate of the ion-acoustic wave. The integrated energies from the two time periods are expressed as percent reflectivities of the incident beam power due to SRS and plotted in Fig. 3. A similar analysis has been done for backscattered light between 350.5 and 352 nm, which is interpreted as SBS backscatter and plotted in Fig. 4. In the integrated data it is clear that late time SRS reflectivities are approximately proportional to the impurity concentration for all concentrations studied. The early time reflectivities are proportional to concentration up to 10% and become independent, or a mildly decreasing function, of concentration between 10% and 30%. Because the ion acoustic damping rate is expected to be linear with impurity concentration in this case [22] a linear dependence of reflectivity on impurity concentration is interpreted as a linear dependence on the damping of the ion acoustic wave. The possibility that dependence of the reflectivity on ion-wave damping is actually the result of suppression of SRS by large amplitude ion waves generated by SBS (as discussed in Refs. [3,4] and references therein) is ruled out by interpreting the SBS reflectivity as a measure of ion-wave amplitude. Note in Fig. 4 that the measured SBS reflectivity and hence ion-wave amplitude does not decrease monotonically with impurity concentration. Rather, in the case of early time and 3% to 10% impurity concentration where the SRS is increasing proportional to concentration and has a similar time dependence to the SBS, the SBS stays constant (within the $\pm 30\%$ error bars). Similarly, in the late time data the SBS is actually increasing with impurity concentration in this range, indicating that the SRS is not reduced at low impurity concentration by large amplitude ion waves. The SBS is observed to be larger late in time, most likely because the electron temperature is low late in time. A similar time dependence was interpreted as "seeding" of the SBS by the LDI generated ion waves in other experiments [5]; however, because the waves are rapidly damped and the SBS growth rates are large in this case, it seems unlikely that the early time LDI could be seeding the SBS 0.5 ns later. These observations are the first demonstration of the direct dependence of SRS reflectivity on the damping rate of the ion acoustic wave. In particular, the early time reflectivity for concentrations between 1% and 10% demonstrates SRS increasing with ion-wave damping when the electron-ion collision rate, electron temperature, radiated power, and SBS level are essentially constant.

A simple model is presented to show how the observed dependence of the reflectivity on ion-wave damping may be explained by secondary decay of the Langmuir wave. In this model the intensity profile of the beam and filamentation are neglected for simplicity, and the Langmuir wave amplitude is assumed to be in the vicinity of the threshold for the secondary decay. This threshold for decay, expressed in terms of the density fluctuation, is given by Ref. [9] for LDI and by Ref. [13] for EDI:

$$\left(\frac{\delta n}{n}\right)_{\mathrm{EDI}} = 4k_L\lambda_D\left(\frac{\nu_{ia}}{\omega_{ia}}\right)^{1/2}\left(\frac{\nu_{\mathrm{em}}}{\omega_p}\right)^{1/2}. \quad (1a)$$

$$\left(\frac{\delta n}{n}\right)_{\mathrm{LDI}} = 4k_L\lambda_D\left(\frac{\nu_{ia}}{\omega_{ia}}\right)^{1/2}\left(\frac{\nu_L}{\omega_p}\right)^{1/2}, \quad (1b)$$

where k_L is the wave vector of the SRS generated Langmuir wave, ν_{ia}/ω_{ia} is the normalized linear ion-wave damping rate, ν_{em} is the linear damping rate of the secondary electromagnetic wave, ν_L is the linear damping rate of the secondary Langmuir wave, and λ_D is the electron Debye length. The measured SRS light is interpreted as Thomson scattering off density fluctuations in the scattering volume using the following assumptions. For these experiments the rapid collisional absorption rate of the incident and reflected light determines the size of the interaction region that can be viewed by the backscatter diagnostic. The effective length L used is the depth at which the attenuation of an incident 351 nm light times the attenuation of the reflected 580 nm light is equal to $1/e$ The length L is 300 μm in this case indicating that the observed SRS comes primarily from the plasma at radii larger than 1 mm. For perfectly coherent fluctuations the reflectivity is proportional to this length to the second power [10]; however, the finite spectral width observed in Fig. 2 ($\Delta k \sim 5.6 \times 10^5$ m^{-1}) indicates that in this experiment the maximum distance over which the radiation can be coherent is given by $\ell_{c\ \mathrm{max}} = 1/\Delta k$. A finite correlation length will reduce the reflectivity by a factor of at least $\ell_{c\ \mathrm{max}}/L$ [8] below the value for coherent fluctuations, giving the maximum reflectivity for a uniform beam as

$$R_{\mathrm{max}} = \frac{1}{4}\left(\frac{n}{n_{c0}}\right)^2 k_0^2 L(\Delta k)^{-1}\left(\frac{\delta n}{n}\right)^2, \quad (2)$$

where k_0 and n_{c0} are the wave number and critical density of the incident beam. This model indicates that the SRS reflectivity is linearly proportional to ion-wave damping if the Langmuir wave amplitude does not grow significantly above the secondary decay threshold. This linear dependence is most clearly observed in the reflectivity

data taken at early time when the impurity concentration is less than 10%. For impurity concentrations above 10% the early time reflectivity is not very dependent on the ion-wave damping. This is likely due the convective saturation of the SRS generated Langmuir wave before it reaches the secondary decay threshold. The secondary decay mechanism will determine only the SRS reflectivity when the primary three wave process is sufficiently strong to drive the Langmuir wave amplitude to the threshold for the secondary decay. Thus at early time and high impurity concentration ($>10\%$) the secondary decay threshold is sufficiently high that the SRS reflectivity is likely limited by the convective saturation of the three wave SRS process and is therefore observed to be approximately independent of ion-wave damping. The late time data show linear dependence of the reflectivity on the impurity concentration up to much higher concentration. This may be because at late time the plasma has cooled and therefore has a higher convective saturation level for the three wave process, resulting in reflectivities that follow the linear scaling with ion-wave damping up to at least 30%, as shown in Fig. 3. However, quantitative analysis of the late time data is complicated by variations of the plasma properties in time and space.

As an additional check of the model of secondary decay, the density perturbation is estimated from the measured reflectivity at early time using Eq. (2), and is compared with that predicted by Eqs. (1a) and (1b). To evaluate Eqs. (1a) and (1b) the damping rates [23] of the Langmuir and electromagnetic waves are calculated using the distribution function expected in a high-Z plasma illuminated with high intensity light [24]. The thresholds are evaluated assuming the average beam intensity (3.0×10^{15} W/cm^2) exists throughout the interaction region, and are shown as solid and dashed lines in Fig. 3. In this case the equilibrium distribution is a super-Gaussian with $n = 3.45$ (where $n = 2$ corresponds to a Maxwellian). The estimate shown for the EDI threshold is not changed significantly by inhomogeneities in the beam profile (i.e., hot spots), but the estimate for LDI may be significantly reduced by inhomogeneities. This reduction results from the fact that the Langmuir wave Landau damping is strongly sensitive to intensity, as discussed in Ref. [23], so that in a hot spot both the threshold density fluctuation will be much lower and the gain of the three wave SRS process will be much higher. As a result in a nonuniform beam LDI may be significantly affecting the SRS even when the reflectivity is well below the uniform beam threshold. Comparison of these estimates with data indicates that the average fluctuation amplitudes observed in the experiment at early times and when the impurity concentration is between 0% and 10% are large enough to excite EDI over much of the beam profile and LDI in intense regions of the beam.

In conclusion, we have observed that the SRS reflectivity in a high-Z plasma is dependent on the ion-wave damping when the Langmuir wave properties are held constant, implying that SRS is limited by a process involving ion acoustic waves. Furthermore, the observed reflectivities are linear with ion-wave damping as expected when the electron wave amplitude is limited by EDI or LDI, and the observed wave amplitudes are near or above the thresholds for those instabilities, indicating that the reflectivity is limited by the stimulation of ion waves by the Langmuir wave.

The authors gratefully acknowledge conversations with D. F. DuBois (LANL), W. Rozmus (U. Alberta), R. P. Drake (LLNL), and K. L. Baker (U.C. Davis) on the nature of the LDI and EDI instabilities and acknowledge suggestions by D. Munro (LLNL) and B. H. Wilde (LANL) concerning LASNEX modeling. Work performed under the auspices of the U.S. Department of Energy by the Lawrence Livermore National Laboratory under Contract No. W-7405-Eng-48.

[1] J. Lindl, Phys. Plasmas **2**, 3933 (1995).
[2] W. L. Kruer, *The Physics of Laser Plasma Interactions* (Addison-Wesley Publishing Co., Redwood City, CA, 1988).
[3] C. J. Walsh, D. M. Villeneuve, and H. A. Baldis, Phys. Rev. Lett. **53**, 1445 (1984).
[4] H. A. Baldis *et al.*, Phys. Rev. Lett. **62**, 2829 (1989).
[5] H. A. Rose, D. F. DuBois, and B. Bezzerides, Phys. Rev. Lett. **58**, 2547 (1987).
[6] K. Estabrook, W. L. Kruer, and M. G. Haines, Phys. Fluids B **1**, 1282 (1989).
[7] T. Kolber, W. Rozmus, and V. T. Tikhonchuk, Phys. Fluids B **5**, 138 (1993).
[8] T. Kolber, W. Rozmus, and V. T. Tikhonchuk, Phys. Plasmas **2**, 256 (1995).
[9] S. J. Karttunen, Phys. Rev. A **23**, 2006 (1981).
[10] J. A. Heikkinen and S. J. Karttunen, Phys. Fluids **29**, 1291 (1986).
[11] R. P. Drake and S. H. Batha, Phys. Fluids B **3**, 2936 (1991).
[12] B. Bezzerides, D. F. DuBois, and H. A. Rose, Phys. Rev. Lett. **70**, 2569 (1993).
[13] K. L. Baker, Ph.D. dissertation, University of California, Davis, 1996; see also P. K. Shukla *et al.*, Phys. Rev. A **27**, 552 (1983).
[14] R. K. Kirkwood *et al.* (to be published).
[15] J. C. Fernandez *et al.*, preceding Letter, Phys. Rev. Lett. **77**, 2702 (1996).
[16] D. H. Kalantar *et al.*, Phys. Plasmas **2**, 3161 (1995).
[17] C. A. Back *et al.* (to be published).
[18] G. Zimmerman and W. Kruer, Comments Plasma Phys. Control. Fusion **2**, 85 (1975).
[19] J. D. Moody *et al.*, Bull. Am. Phys. Soc. **39**, 1753 (1994).
[20] H. N. Kornblum, R. L. Kauffman, and J. A. Smith, Rev. Sci. Instrum. **57**, 2179 (1986).
[21] R. K. Kirkwood *et al.*, Bull. Am. Phys. Soc. **39**, 1753 (1994); Rev. Sci. Inst. (to be published).
[22] E. A. Williams *et al.*, Phys. Plasmas **2**, 129 (1995).
[23] B. B. Afeyan, A. E. Chou, and W. L. Kruer (to be published).
[24] P. Alaterre, J.-P. Matte, and M. Lamoureaux, Phys. Rev. A **34**, 1578 (1986); A. B. Langdon, Phys. Rev. Lett. **44**, 575 (1980).